

Linear Induction Motor Sensorless Speed Control Based on T-S Fuzzy Design ^{*}

Kuang-Yow Lian ^{*} Cheng-Yao Hung ^{**} Chian-Song Chiu ^{**}

^{*} Department of Electrical Engineering, National Taipei University of Technology, Taipei 10608, Taiwan (e-mail: kylian@ntut.edu.tw).

^{**} Department of Electrical Engineering, Chung-Yuan Christian University, Chung-Li 32023, Taiwan (e-mail: g9102804@cycu.edu.tw; cschiu@dec.ee.cycu.edu.tw)

Abstract: In this paper, a sensorless speed control for linear induction motors (LIMs) is developed based on fuzzy observer design. First, the LIMs is represented by a Takagi-Sugeno (T-S) fuzzy model. Next, the fuzzy observer is constructed to estimate the immeasurable states of mover speed and secondary flux, where the observer gains are obtained by solving a set of linear matrix inequalities (LMIs). To overcome the high nonlinearity, a two stage approach is applied to design the control law. Then, exponential convergence for both estimation error and tracking error is concluded. This indicates that the proposed sensorless controller possesses the feature of fast transient response and high robustness. Finally, simulations and experiments are carried out to verify the theoretical results and show satisfactory performance.

1. INTRODUCTION

The linear induction motor (LIM) has many excellent performance features such as high starting thrust force, alleviation of gear between motor and the motion devices, reduction of mechanical losses and the size of motion devices, silence, and so on (Boldea et al. [1997], Abdou et al. [1991]). Due to the advantages motioned above, the LIM are widely used in many industrial applications, including transportation, conveyor systems, actuators, and material handling, with satisfactory performance. For advanced industrial application, the requirements of speed transducers such as a linear encoder or a resolver are necessary for feedback systems on applications of motion control. However, these requirements not only increase the cost, weight, and complexity but also degrade the robustness and reliability of the system. The mechanical sensors can be avoided when sensorless control strategies are adopted. The research of sensorless control for LIM is beneficial because of the elimination of feedback wiring, reduced cost, and improved reliability.

In the present age, T-S fuzzy model (Takagi et al. [1985]) has been extensively studied because it can represent a nonlinear system using some fuzzy rules and be easily incorporated with conventional control methods. In T-S fuzzy model, the nonlinear system can be decomposed into several linear subsystems. Then, the control problem becomes easier to handle because it is to find the corresponding local linear compensators for each subsystem to achieve the desired objective. This is the major advantage of T-S fuzzy model. The stability analysis of a T-S fuzzy system is to look for a common positive definite matrix P satisfying global *Lyapunov function* $V(x) = x^T P x > 0$

and $\dot{V}(x) < 0$ for all subsystems (Lian et al. [2006]). However, it is a difficult work to find such a matrix. There are a series of methods that have been developed to solve the matrix P . The LMI method is an effective one and can be solved rapidly by using software tools such as Matlab (Tanaka et al. [2000]). Then, the parameters of the observer can be obtained by solving the LMIs.

In this paper, we propose a novel speed sensorless control for the full fifth-order model of LIM based on the fuzzy observer design to estimate the immeasurable variables of mover speed and secondary flux. Membership functions fitting this property can be proven that estimation errors converge to zero exponentially. After the fuzzy observer has been designed, the speed tracking controller is separately developed, i.e., the estimation error is assumed zero in controller design. In details, we first formulate the speed tracking control into a force tracking problem (Lian et al. [2005]). In the design process, a skew-symmetric property pertaining to the dynamics of the LIM is utilized to simplify the structure of the controller. Using this controller, the tracking error can converges to zero exponentially. The feature of exponential convergence for both the estimation and tracking errors shows the fast transient response and high robustness. To demonstrate the effectiveness of the proposed scheme, a voltage-fed drive system is used as an example to achieve speed tracking. Even considering load uncertainties, the simulation and experimental results still achieve good performance.

2. DYNAMICAL MODEL OF LIMs

Denoting the state vectors $\mathbf{i} = [i_{pa} \ i_{pb}]^T$, $\lambda = [\lambda_{sa} \ \lambda_{sb}]^T$, and $\mathbf{V}_p = [V_{pa} \ V_{pb}]^T$, the fifth-order dynamic model of the LIM in *a-b* stationary reference frame is described by the following vector compact form (Boldea et al. [1997]):

^{*} This work was supported by the National Science Council, Taiwan, R.O.C., under Grant NSC 93-2213-E-033-008 and 96-2213-E-033-077.

$$\dot{\mathbf{i}} = -\gamma \mathbf{i} - \left(\frac{\pi n_p L_m}{\sigma \ell L_s} v_m \mathbf{J}_2 - \frac{L_m R_s}{\sigma L_s^2} \mathbf{I}_2 \right) \lambda + \frac{1}{\sigma} \mathbf{V}_p \quad (1)$$

$$\dot{\lambda} = \frac{L_m R_s}{L_s} \mathbf{i} + \left(\frac{\pi n_p}{\ell} v_m \mathbf{J}_2 - \frac{R_s}{L_s} \mathbf{I}_2 \right) \lambda \quad (2)$$

$$\dot{v}_m = \frac{F}{M} - \frac{F_l}{M} - \frac{D}{M} v_m \quad (3)$$

where

$$\mathbf{I}_2 = \begin{bmatrix} 1 & 0 \\ 0 & 1 \end{bmatrix} \text{ and } \mathbf{J}_2 = \begin{bmatrix} 0 & -1 \\ 1 & 0 \end{bmatrix}.$$

Here $\gamma = \left(\frac{R_p}{\sigma} + \frac{L_m^2 R_s}{\sigma L_s^2} \right)$, $\sigma = L_p - \frac{L_m^2}{L_s}$, $F = \kappa \mathbf{i}^\top \mathbf{J}_2 \lambda$, $\kappa = 3\pi n_p L_m / 2\ell L_s$, and

i_{pa} (i_{pb})	a -axis and b -axis primary current
V_{pa} (V_{pb})	a -axis and b -axis primary voltage
λ_{sa} (λ_{sb})	a -axis and b -axis secondary flux
v_m	mover speed
R_p (R_s)	primary (secondary) resistance
L_p (L_s)	primary (secondary) inductance
L_m	mutual inductance
ℓ	pole pitch
M	primary mass
D	viscous friction
n_p	number of pole pairs
F_l	load disturbance
F	electromechanical coupling force
κ	force constant

The longitudinal end-effect is approximated by Taylor's series and can be taken as an external load force

$$F_l = \theta_1 + \theta_2 v_m + \theta_3 v_m^2.$$

This end-effect increases with the speed of the primary (Huang et al. [2007]). The nominal part of the load force can be included in the damping force, and the remainder is formulated as an amount of uncertainty in the system. A rigorous design to deal with the uncertainty using adaptive technique will lead to the mixed problem of simultaneously identifying the parameters and estimating state variables. This will yield complex control law. An alternative is to cope with this small amount of uncertainty by a high robust controller. The controller to be proposed will make the error system exponentially stable and is very robust to uncertainty.

The dynamical model possess a skew-symmetric property in its state equations for unmeasurable variables, which will be used in controller design. To see this, we rearrange the dynamical equations by using more compact notations. Let us denote $\underline{x} = [x_1 \ x_2 \ x_3 \ x_4]^\top = [i_{pa} \ i_{pb} \ \lambda_{sa} \ \lambda_{sb}]^\top$. The model (1)~(3) can be rewritten as

$$Q \dot{\underline{x}} + G(v_m) \underline{x} + R(v_m) \underline{x} = \tau \quad (4)$$

$$M \dot{v}_m + D v_m = F - F_l \quad (5)$$

where

$$Q = \begin{bmatrix} L_s \sigma I_2 & 0 \\ 0 & I_2 \end{bmatrix}, \quad G(v_m) = \begin{bmatrix} 0 & 0 \\ 0 & -J_2 \end{bmatrix} \frac{\pi n_p}{\ell} v_m,$$

$$R(v_m) = \begin{bmatrix} L_s \sigma \gamma I_2 & \frac{\pi n_p L_m}{\ell} v_m J_2 - \frac{L_m R_s}{L_s} I_2 \\ -\frac{L_m R_s}{L_s} I_2 & \frac{R_s}{L_s} I_2 \end{bmatrix},$$

$$\tau = [L_s V_{pa} \ L_s V_{pb} \ 0 \ 0]^\top.$$

Therefore, $G(v_m)$ is a skew-symmetric matrix. The skew-symmetric matrix represents a "workless force" in the

physical sense, which does not affect the energy balance and system stability. Thus, $G(v_m)$ is not needed to be canceled in the control law. This fact will enable the control law to be simplified in Section 4.

3. T-S FUZZY REPRESENTATION OF LIMS

The T-S fuzzy dynamic models, by fuzzy IF-THEN rules, are utilized to exactly represent nonlinear systems in a region of interest. This representation is applied to an LIM.

3.1 Fuzzy Modeling of LIM

To express the LIM (4) and (5) in terms of T-S fuzzy model, we further rewrite the equations in the following form:

$$\begin{aligned} \dot{x}(t) &= A(x) x(t) + B u + b F_l \\ y(t) &= C x(t) \end{aligned} \quad (6)$$

where $x(t) = [x_1 \ x_2 \ x_3 \ x_4 \ x_5]^\top = [i_{pa} \ i_{pb} \ \lambda_{sa} \ \lambda_{sb} \ v_m]^\top$ are the overall states; $y(t) = [i_{pa} \ i_{pb}]^\top$ are the measurable output; $u = [V_{pa} \ V_{pb}]^\top = [u_1 \ u_2]^\top$ are the control input; and the associated matrices and vector:

$$A(x) = \begin{bmatrix} -\gamma & 0 & \frac{L_m R_s}{\sigma L_s^2} & 0 & \frac{\pi n_p L_m}{\sigma \ell L_s} \lambda_{sb} \\ 0 & -\gamma & 0 & \frac{L_m R_s}{\sigma L_s^2} & -\frac{\pi n_p L_m}{\sigma \ell L_s} \lambda_{sa} \\ \frac{L_m R_s}{L_s} & 0 & -\frac{R_s}{L_s} & 0 & -\frac{\pi n_p}{\ell} \lambda_{sb} \\ 0 & \frac{L_m R_s}{L_s} & 0 & -\frac{R_s}{L_s} & \frac{\pi n_p}{\ell} \lambda_{sa} \\ -\frac{\kappa}{M} \lambda_{sb} & \frac{\kappa}{M} \lambda_{sa} & 0 & 0 & -\frac{D}{M} \end{bmatrix},$$

$$B = \begin{bmatrix} \frac{1}{\sigma} & 0 \\ 0 & \frac{1}{\sigma} \\ 0 & 0 \\ 0 & 0 \\ 0 & 0 \end{bmatrix}, \quad b = \begin{bmatrix} 0 \\ 0 \\ 0 \\ 0 \\ -\frac{1}{M} \end{bmatrix}, \quad C = \begin{bmatrix} 1 & 0 \\ 0 & 1 \\ 0 & 0 \\ 0 & 0 \\ 0 & 0 \end{bmatrix}^\top.$$

Then, according to Lian et al. [2006], the T-S fuzzy model representation of (7) can be expressed by the following rules:

Plant Rule i :

IF λ_{sa} is F_{1i} and λ_{sb} is F_{2i} THEN

$$\dot{x}(t) = A_i x(t) + B u(t) + b F_l$$

$$y(t) = C x(t), \quad i = 1, 2, 3, 4 \quad (7)$$

where λ_{sa} and λ_{sb} are premise variables which are immeasurable. The fuzzy sets F_{ji} ($j = 1, 2$) are set as

$$F_{11} = F_{12} = \frac{x_3 - d_1}{D_1 - d_1}; \quad F_{13} = F_{14} = \frac{D_1 - x_3}{D_1 - d_1};$$

$$F_{21} = F_{23} = \frac{x_4 - d_2}{D_2 - d_2}; \quad F_{22} = F_{24} = \frac{D_2 - x_4}{D_2 - d_2}.$$

The system matrices A_i of subsystem i are given by

$$A_i = \begin{bmatrix} -\gamma & 0 & \frac{L_m R_s}{\sigma L_s^2} & 0 & \frac{\pi n_p L_m}{\sigma \ell L_s} \vartheta_i \\ 0 & -\gamma & 0 & \frac{L_m R_s}{\sigma L_s^2} & -\frac{\pi n_p L_m}{\sigma \ell L_s} \varphi_i \\ \frac{L_m R_s}{L_s} & 0 & -\frac{R_s}{L_s} & 0 & -\frac{\pi n_p}{\ell} \vartheta_i \\ 0 & \frac{L_m R_s}{L_s} & 0 & -\frac{R_s}{L_s} & \frac{\pi n_p}{\ell} \varphi_i \\ -\frac{\kappa}{M} \vartheta_i & \frac{\kappa}{M} \varphi_i & 0 & 0 & -\frac{D}{M} \end{bmatrix}$$

where

$$\begin{aligned} \varphi_1 &= D_1, \vartheta_1 = D_2; \varphi_2 = D_1, \vartheta_2 = d_2; \\ \varphi_3 &= d_1, \vartheta_3 = D_2; \varphi_4 = d_1, \vartheta_4 = d_2. \end{aligned}$$

In these fuzzy rules, D_1 and d_1 are the upper bound and lower bound of λ_{sa} , respectively, and D_2, d_2 are the upper bound and lower bound of λ_{sb} , respectively. Using the singleton fuzzifier, product fuzzy inference and weighted average defuzzifier, the final output of the fuzzy system is inferred as follows:

$$\begin{aligned} \dot{\hat{x}}(t) &= \sum_{i=1}^4 \mu_i(x(t)) \{A_i x(t) + Bu(t)\} + bF_l \\ y(t) &= Cx(t), \end{aligned} \quad (8)$$

where $\mu_i(x(t)) = \phi_i(x(t)) / \sum_{i=1}^4 \phi_i(x(t))$ with $\phi_i(x(t)) = \prod_{j=1}^2 F_{ji}(x(t))$. Note that $\sum_{i=1}^4 \mu_i(x(t)) = 1$ for all t , where $\mu_i(x(t)) \geq 0$ for all $i = 1, 2, 3, 4$. Based on the setting of F_{ji} and A_i , it can be checked that the inferred output is exactly equivalent to the model of LIM (6).

3.2 Fuzzy Observer Design

Now, we will design the fuzzy observer to estimate the immeasurable states. According to the fuzzy model (7), the fuzzy observer is given as follows:

Observer Rule i :

$$\begin{aligned} \text{IF } \hat{\lambda}_{sa} \text{ is } F_{1i} \text{ and } \hat{\lambda}_{sb} \text{ is } F_{2i} \text{ THEN} \\ \dot{\hat{x}}(t) &= A_i \hat{x}(t) + Bu(t) + L_i(y(t) - \hat{y}(t)) + bF_l \\ \hat{y}(t) &= C\hat{x}(t), \quad i = 1, 2, 3, 4 \end{aligned} \quad (9)$$

where the premise variables $\hat{\lambda}_{sa}$ and $\hat{\lambda}_{sb}$ are accordingly the estimations of λ_{sa} and λ_{sb} , respectively; $\hat{x}(t)$ and $\hat{y}(t)$ denote the estimations of $x(t)$ and $y(t)$, respectively; and L_i is an observer gain to be determined. The inferred output of the observer is

$$\begin{aligned} \dot{\hat{x}}(t) &= \sum_{i=1}^4 \mu_i(\hat{x}(t)) \{A_i \hat{x}(t) + Bu(t) + L_i(y(t) - \hat{y}(t))\} \\ &\quad + bF_l \\ \hat{y}(t) &= C\hat{x}(t). \end{aligned} \quad (10)$$

Define the state estimation error $e(t) = x(t) - \hat{x}(t)$. Subtracting (8) by (10), we have

$$\dot{e}(t) = \sum_{i=1}^4 \mu_i(\hat{x}(t)) \{(A_i - L_i C)e\} + l(t)$$

where

$$l(t) = \sum_{i=1}^4 (\mu_i(x) - \mu_i(\hat{x})) \{A_i x(t)\} \quad (11)$$

The uncertainty term $l(t)$ in (11) arises due to immeasurable premise variables λ_{sa} and λ_{sb} . To make the effect of the uncertainty be vanished, a closer investigation is addressed now. We notice that the membership functions $F_{ij}(\cdot)$ satisfy $F_{ij}(x(t)) - F_{ij}(\hat{x}(t)) = \eta_{ij}(x(t) - \hat{x}(t))$ for some bounded function vector η_{ij} . According to the grade function $\mu_i(x(t)) = F_{1i}(x) F_{2i}(x)$, we have

$$\begin{aligned} \mu_i(x(t)) - \mu_i(\hat{x}(t)) &= \eta_{1i}(x - \hat{x})F_{2i}(x) + F_{1i}(\hat{x})\eta_{2i}(x - \hat{x}) \\ &= (\eta_{1i}F_{2i}(x) + \eta_{2i}F_{1i}(\hat{x}))(x - \hat{x}) \\ &\equiv \Lambda_i(x(t) - \hat{x}(t)) \end{aligned}$$

for some bounded function vector Λ_i .

In light of this property, we have

$$l(t) = \left(\sum_{i=1}^4 A_i x(t) \Lambda_i \right) e.$$

Supposed that $x(t)$ is bounded (this will be confirmed in controller design given later), the uncertainty $l(t)$ satisfies the bound

$$l^T l \leq e^T U^T U e \quad (12)$$

with a symmetric positive-definite matrix U . This undesired term $l(t)$ will affect the estimation performance. However, by suitably choosing observer gains L_i , its effect can be exponentially attenuated to zero. Now, we apply Lyapunov method to get the observer gains L_i , for $i = 1, 2, 3, 4$.

Choose the Lyapunov function candidate $V_o(e(t)) = e^T(t) P e(t)$. Taking the time derivative, we have

$$\begin{aligned} \dot{V}_o(e) &= \sum_{i=1}^4 \mu_i(\hat{x}) e^T \left[(A_i - L_i C)^T P + P(A_i - L_i C) \right] e \\ &\quad + l^T P e + e^T P l. \end{aligned}$$

From (12), $l^T P e \leq e^T U^T P e$ and hence

$$l^T P e + e^T P l \leq e^T (U^T P + P U) e.$$

Therefore, the inequality for $\dot{V}_o(e)$ can be expressed as follows:

$$\dot{V}_o(e) \leq \sum_{i=1}^4 \mu_i(\hat{x}) e^T G_i e - e^T E P E e \quad (13)$$

where $G_i = (A_i - L_i C)^T P + P(A_i - L_i C) + U^T P + P U + E P E$. The symmetric positive-definite matrix E is introduced to dominate the estimation convergence rate. The first term in (13) is negative definite if the following LMIs for $P > 0$ and Z_i hold

$$\begin{aligned} A_i^T P + P A_i - C^T Z_i^T - Z_i C + U^T P + P U + E P E < 0, \\ \forall i = 1, 2, 3, 4, \end{aligned} \quad (14)$$

where $Z_i = P L_i$. Then, (13) is shown to be negative definite as follows:

$$\dot{V}_o(e) \leq -e^T E P E e,$$

which implies that $\hat{x}(t)$ converges to $x(t)$ exponentially, if $x(t)$ is bounded.

Design of the Fuzzy Observer: For the fuzzy observer (9), suppose that all states and control input are bounded. If there exists a common positive definite matrix P and Z_i such that the LMIs (14) are feasible, then the estimation error converges to zero exponentially by letting observer gains $L_i = P^{-1} Z_i$.

We can solve LMIs (14) using powerful packages like Matlab LMI Toolbox to obtain P and Z_i . In turn, the observer gains are calculated from $L_i = P^{-1} Z_i$.

4. CONTROLLER DESIGN

Due to the exponential convergence of estimation error, we directly use $\lambda(t)$ and $v_m(t)$ instead of $\hat{\lambda}(t)$ and $\hat{v}_m(t)$,

respectively to carry out the following controller design. This treatment can simplify the design procedure.

4.1 Mechanical Loop Control

First, denote the speed tracking error as $\tilde{v}_m \equiv v_m - v_d$. The tracking error dynamics can be rewritten as

$$M\dot{\tilde{v}}_m + (D + k_v)\tilde{v}_m = F - F_d + (F_d - Y\theta + k_v\tilde{v}_m),$$

where F_d denotes the desired force producing the desired speed; k_v is an adjustable damping ratio; $Y = [1 \ v_m \ v_m^2 \ v_d \ \dot{v}_d]$ is the regression vector; and $\theta = [\theta_1 \ \theta_2 \ \theta_3 \ D \ M]^T$ is the parameter vector. For speed tracking control, the desired force is selected as

$$F_d = Y\theta - k_v\tilde{v}_m.$$

This yields the following error dynamics

$$M\dot{\tilde{v}}_m + (D + k_v)\tilde{v}_m = F - F_d \quad (15)$$

If $F - F_d$ is driven to zero, the mover speed will converge to the desired value. Therefore, the speed tracking control problem can be reformulated into the force tracking problem.

4.2 Electrical Loop Control

According to (Lian et al. [2006]), the desired flux and current are designed below in which some mathematical process are omitted:

$$\begin{bmatrix} x_{3d} \\ x_{4d} \end{bmatrix} = \begin{bmatrix} c \cos(\rho(t)) \\ c \sin(\rho(t)) \end{bmatrix}, \quad (16)$$

$$\begin{bmatrix} x_{1d} \\ x_{2d} \end{bmatrix} = \frac{1}{L_m} \left(\frac{L_s}{R_s} \left(\dot{\rho} - \frac{\pi n_p}{\ell} v_m \right) J_2 + I_2 \right) \begin{bmatrix} x_{3d} \\ x_{4d} \end{bmatrix} + \frac{\kappa L_s}{L_m R_s} \tilde{v}_m J_2 \begin{bmatrix} x_1 \\ x_2 \end{bmatrix}. \quad (17)$$

with the angle $\rho(t)$

$$\dot{\rho}(t) = \frac{\pi n_p}{\ell} v_m + \frac{L_m R_s}{\kappa L_s c^2} F_d - \frac{\kappa}{c^2} \tilde{v}_m (x_1 x_{3d} + x_2 x_{4d}),$$

Finally, the control law is formulated as follows:

$$\begin{bmatrix} u_1 \\ u_2 \end{bmatrix} = \sigma \begin{bmatrix} \dot{x}_{1d} \\ \dot{x}_{2d} \end{bmatrix} + \sigma \gamma \begin{bmatrix} x_{1d} \\ x_{2d} \end{bmatrix} + \frac{\rho}{L_s} I_2 \begin{bmatrix} \tilde{x}_1 \\ \tilde{x}_2 \end{bmatrix} - \frac{\pi n_p L_m}{\ell L_s} v_m J_2 \begin{bmatrix} \tilde{x}_3 \\ \tilde{x}_4 \end{bmatrix} + \left(\left(\frac{\pi n_p L_m}{\ell L_s} v_m - \frac{\kappa}{L_s} \tilde{v}_m \right) J_2 - \frac{L_m R_s}{L_s^2} I_2 \right) \begin{bmatrix} x_{3d} \\ x_{4d} \end{bmatrix} \quad (18)$$

The control architecture for a sensorless LIM is shown in Fig. 1. The implementation of the control law (18) is complicated due to the first term on the right-hand side, which includes the time derivative of x_{1d} and x_{2d} . Fortunately, the exponential stability shown in the following section make the controller very robust to uncertainty. This feature allows the approximation $\dot{x}_{id} \approx x_{id} - \bar{x}_{id}$, where $\dot{\bar{x}}_{id} + \bar{x}_{id} = x_{id}$. The simplified control law will be adopted in our experiment.

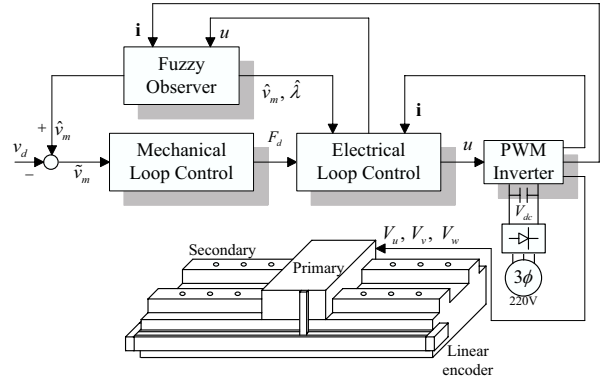


Fig. 1. The concept of control design for sensorless LIM.

4.3 Stability Analysis

Here we define the error signal for the electrical part as $\tilde{\underline{x}} = \underline{x} - \underline{x}_d$, where $\underline{x}_d = [x_{1d} \ x_{2d} \ x_{3d} \ x_{4d}]^T$. The control objective of steering F to track F_d can be achieved if $\tilde{\underline{x}} \rightarrow 0$. To this end, the equation (4) is rewritten in terms of $\tilde{\underline{x}}$ as

$$Q\dot{\tilde{\underline{x}}} + G(v_m)\tilde{\underline{x}} + R(v_m)\tilde{\underline{x}} = \xi_p + \bar{\xi}_p \quad (19)$$

where ξ_p is the perturbed term

$$\xi_p = \tau - [Q\dot{\underline{x}}_d + G(v_m)\underline{x}_d + R(v_m)\underline{x}_d] - \bar{\xi}_p. \quad (20)$$

and

$$\bar{\xi}_p = -\bar{R}_2\tilde{\underline{x}} - \kappa\tilde{v}_m [-x_{4d} \ x_{3d} \ x_2 \ -x_1]^T$$

Thus, the desired flux and current is obtained once $\xi_p = 0$ is satisfied.

For system stability analyze, the Lyapunov function candidate is chosen as follows:

$$V_c(\tilde{\underline{x}}(t), \tilde{v}_m) = \frac{1}{2}\tilde{\underline{x}}^T(t) Q\tilde{\underline{x}}(t) + \frac{1}{2}M\tilde{v}_m^2.$$

The time derivative of V_c , we obtain

$$\dot{V}_c(\tilde{\underline{x}}(t), \tilde{v}_m) = -\tilde{\underline{x}}^T \bar{R}_1 \tilde{\underline{x}} - (D + k_v)\tilde{v}_m^2.$$

where

$$\bar{R}_1 = \begin{bmatrix} L_s \sigma \gamma I_2 + \rho I_2 - \frac{L_m R_s}{L_s} I_2 \\ -\frac{L_m R_s}{L_s} I_2 & \frac{R_s}{L_s} I_2 \end{bmatrix},$$

$$\bar{R}_2 = \begin{bmatrix} -\rho I_2 & \frac{\pi n_p L_m}{\ell} v_m J_2 \\ 0 & 0 \end{bmatrix}.$$

It can be checked that the tracking error converges to zero exponentially once $\bar{R}_1 > 0$ by choosing $\rho > -L_s R_p$.

5. SIMULATION AND EXPERIMENTAL RESULTS

To further verify the validity of the proposed scheme, several experiments of speed control are described in this section. The experimental setup is shown in Fig. 2. In our experiments, the developed controller is realized by a DSP-based control card (Simu-Drive system), which takes the TMS320F2812 DSP (fixed-point 32-bit) as the main control core. The DSP control card also provides multichannel of A/D and encoder interface circuits. Here, three-phase voltages and currents are sampled by the A/D converters and fed into the DSP-based controller. The speed is measured by a linear encoder with precision $20\mu\text{m}$ for one pulse. The speed signal is only used to verify the precision of the estimated speed and is not fed

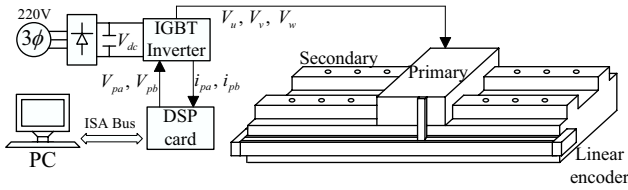


Fig. 2. The experimental setup.

into the controller. In addition, the block-building Matlab Simulink Toolbox and Real-Time Workshop are taken as an interface between software and hardware. When the build-up controller block is established, the Real-Time Workshop plays a role of a compiler to transform the controller into a C code, which is download to the DSP-based control card. The specifications and parameters of the LIM are listed in Table 1. The speed control parameters are chosen as follows: $k_v = 1000$, $c = 0.55$, and $\rho = 0.9$. According to LMI (14), where we let $U = \text{diag}\{0.9, 1.9, 0.1, 0.04, 8.9\}$ and $E = \text{diag}\{12, 12, 0.01, 0.01, 1.9\}$. The observer gains solved from the LMI toolbox of Matlab, whereas they are not shown due to space consideration. Based on this setting, the following speed control experiments are performed.

TABLE 1
 THE SPECIFICATION AND PARAMETERS OF THE LIM

RATED SPECIFICATION	
POLE PAIR	2
POWER	1 HP
VOLTAGE	240 V
CURRENT	5 A
POLE PITCH	0.0465 m
SECONDARY LENGTH	0.82 m
PARAMETERS	
R_p	13.2 Ω
R_s	11.78 Ω
L_p	0.42 H
L_s	0.42 H
L_m	0.4 H
M	4.775 kg
D	53 kg/s

Speed Regulation: Consider a speed regulation $v_d = 0.5\text{m/sec}$.

Simulation result: The desired and actual speed, actual and estimated speed are shown in Figs. 3(a) and 3(b), respectively. The speed estimation error is shown in Fig. 3(c).

Experimental result: The desired and actual speed, actual and estimated speed are shown in Figs. 4(a) and 4(b), respectively. The speed estimation error is shown in Fig. 4(c). The primary voltage of u -phase V_u and primary current of u -phase i_u are shown in Figs. 5(a) and 5(b), respectively. Furthermore, the desired and estimation secondary flux of one phase are shown in Fig. 5(c).

Consider a speed regulation $v_d = 0.3\text{m/sec}$ with an abrupt external force variation. To generate such external force in this experiment, an 1kg load is placed gently on the moving table during operating process. The external force is added at $t = 1\text{sec}$ and removed at $t = 1.6\text{sec}$. The experimental results for the desired and actual speed,

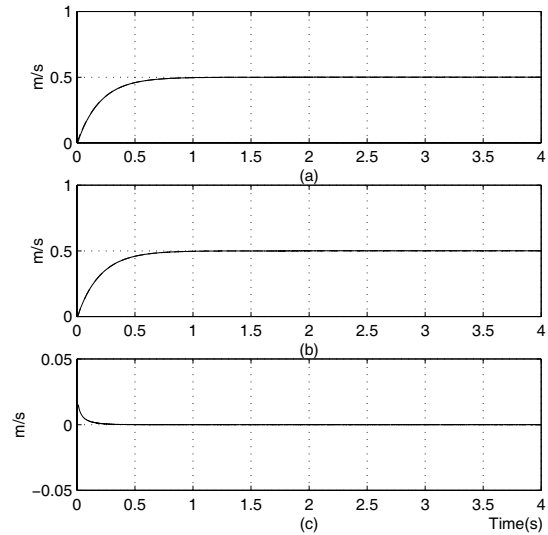


Fig. 3. Simulation results of speed regulation, (a) desired speed (---) and actual speed (—), (b) estimated speed (---) and actual speed (—), (c) speed estimation error.

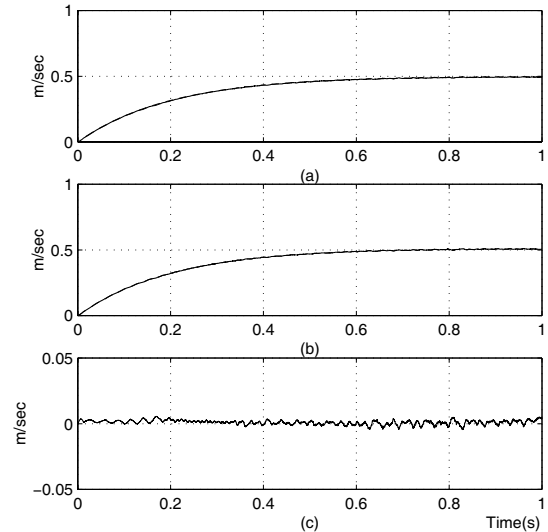


Fig. 4. Experimental results of speed regulation, (a) desired speed (---) and actual speed (—), (b) estimated speed (---) and actual speed (—), (c) speed estimation error.

actual and estimated speed are shown in Figs. 6(a) and 6(b), respectively. The speed estimation error is shown in Fig. 6(c). The primary voltage of u -phase V_u and primary current of u -phase i_u are shown in Figs. 7(a) and 7(b), respectively.

From these figures, we can find that the estimation errors and the tracking errors have good convergence rate.

6. CONCLUSIONS

This paper has presented a sensorless speed control scheme for LIM based on the T-S fuzzy model. The T-S fuzzy observer algorithm has been used to estimate the mover speed and secondary flux of a LIM, where the observer gains are obtained by solving a set of LMIs. The two-stage design technique is applied to construct the controller for

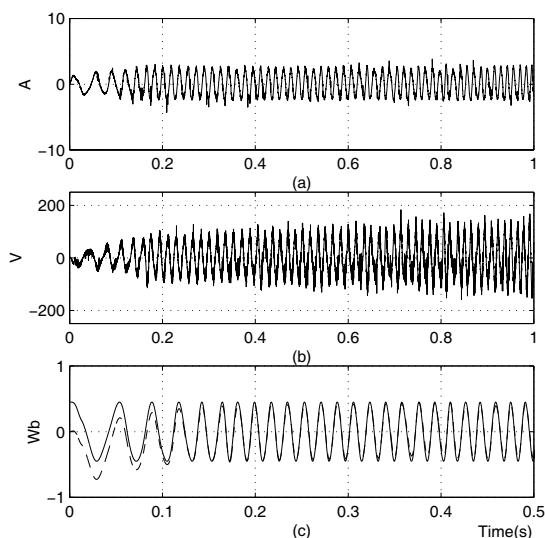


Fig. 5. Experimental results of speed regulation, (a) primary current of u -phase i_u , (b) primary voltage of u -phase V_u , and (c) estimated (---) and desired (—) secondary fluxes λ_{sa} .

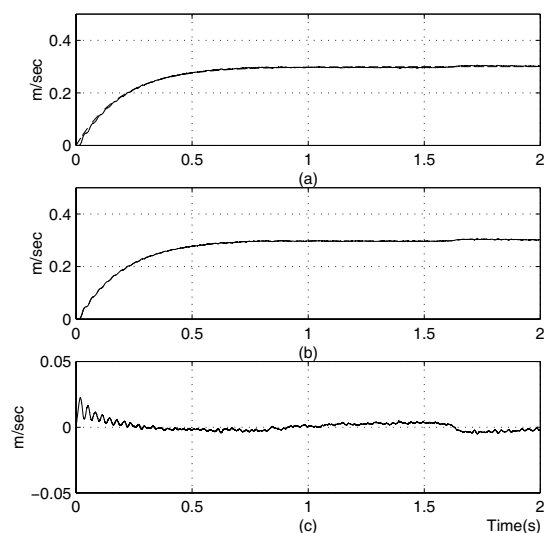


Fig. 6. Experimental results of speed regulation with abrupt load variation, (a) desired speed (---) and actual speed (—), (b) estimated speed (---) and actual speed (—), (c) speed estimation error.

speed tracking purpose. From the experimental results, we found that good transient responses are obtained, and the speed tracking errors approximate to zero in steady state. One more thing that deserves to be mentioned is that the stability discussed in this paper is exponentially stable. This means that the system with our proposed control method is very robust with uncertainties.

REFERENCES

- I. Boldea and S. A. Nasar. *Linear Electric Actuators and Generators*. Cambridge, U.K.: Cambridge Univ. Press, 1997.
- G. H. Abdou and S. A. Sherif. Theoretical and experimental design of LIM in automated manufacturing systems. *IEEE Trans. Ind. Applications*, vol. 27, no. 2, pp. 286-293, Mar./Apr. 1991.

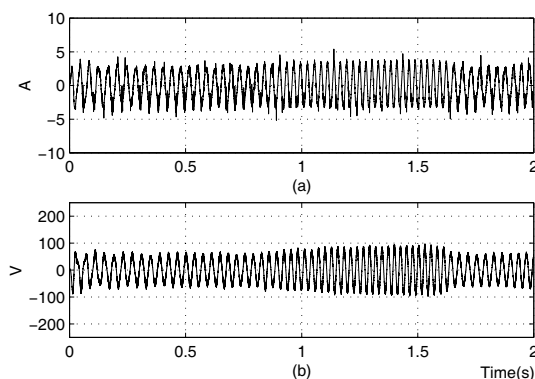


Fig. 7. Experimental results of speed regulation with abrupt load variation, (a) primary current of u -phase i_u and (b) primary voltage of u -phase V_u .

- T. Takagi and M. Sugeno. Fuzzy identification of system and its applications to modeling and control. *IEEE Trans. Syst., Man, Cybern.*, vol. SMC-15, no. 1, pp. 116-132, 1985.
- K. Y. Lian and J. J. Liou. Output tracking control for fuzzy systems via output feedback design. *IEEE Trans. Fuzzy syst.*, vol. 14, no. 5, pp. 628-639, Oct. 2006.
- K. Tanaka and H. O. Wang. *Fuzzy Control Systems Analysis and Design: A Linear Matrix Inequality Approach*. New York: Wiley, 2000.
- K. Y. Lian, C. Y. Hung, C. S. Chiu, and P. Liu. Induction motor control with friction compensation: an approach of virtual-desired-variable synthesis. *IEEE Trans. Power Electronics*, vol. 20, no. 5, pp. 1066-1074, Sep. 2005.
- C. I. Huang and L. C. Fu. Adaptive approach to motion controller of linear induction motor with friction compensation. *IEEE/ASME Transactions on Mechatronics*, vol. 12, no. 4, pp. 480-490, August 2007.